

Original Research

Characterization of Extracellular Vesicles by Sulfophosphovanillin Colorimetric Assay and Raman Spectroscopy

Alexey Senkovenko^{1,2}, Gleb Skryabin³, Evgeniia Parshina², Alexey Piryazev^{4,5},
Elena Tchevkina^{3,*}, Dmitry Bagrov^{2,3,*}¹Institute for Regenerative Medicine, Sechenov University, 119991 Moscow, Russia²Faculty of Biology, Lomonosov Moscow State University, 119234 Moscow, Russia³Institute of Carcinogenesis, N.N. Blokhin National Medical Research Center of Oncology, 115478 Moscow, Russia⁴Faculty of Chemistry, Lomonosov Moscow State University, 119234 Moscow, Russia⁵Research Center for Genetics and Life Sciences, Sirius University of Science and Technology, 354340 «Sirius» Federal Territory, Russia*Correspondence: tchevkina@mail.ru (Elena Tchevkina); bagrov@mail.bio.msu.ru (Dmitry Bagrov)

Academic Editor: Graham Pawelec

Submitted: 8 June 2024 Revised: 9 September 2024 Accepted: 12 September 2024 Published: 23 October 2024

Abstract

Background: Detailed characterization of extracellular vesicles (EVs) is crucial for their application in medical diagnostics. However, the complexity of their chemical composition and the heterogeneity of EV populations make their characterization challenging. Here we describe two analytical procedures that can help overcome this challenge. **Methods:** Small EVs were isolated from conditioned cell culture media using ultracentrifugation and characterized using nanoparticle tracking analysis (NTA) and transmission electron microscopy (TEM). Raman spectroscopy was used to assess the overall composition of the isolated samples and lipids extracted from them. Sulfophosphovanillin (SPV) colorimetric assay was used to quantify the contents of lipid. **Results:** Six samples of EVs were characterized. The lipid contents measured using SPV assay was in reasonable agreement with the quantitative estimates based on the particle size and concentration measured using NTA. The most peaks observed in the Raman spectra could be attributed to either proteins or lipids, and their origins was confirmed by lipid extraction. The protein-to-lipid ratio was estimated based on the Raman spectra. **Conclusions:** The experiential procedures described in this study will help to overcome the challenge of quick and highly informative characterization of the EVs.

Keywords: extracellular vesicles; optical measurement; lipid concentration; optical assay; Raman spectroscopy

1. Introduction

Extracellular vesicles (EVs) are membrane-surrounded particles secreted by cells into the extracellular space. Their key function is intercellular communication; they deliver nucleic acids, proteins, lipids and small-molecule metabolites between cells. The molecular composition of vesicles, including the lipid-protein composition of EV membranes, largely determines the fate of secreted vesicles in body fluids as well as their functional activity. Analysis of their biochemical composition can help to diagnose many diseases, including cancer [1,2]. Besides, control of their biochemical composition is necessary for their application in regenerative medicine and drug delivery [3]. However, samples of EVs isolated from cell culture media and body fluids are prone to various contaminations [4–6]. Thus, assessment of their purity and composition is crucial.

Optical measurements lay the technical foundation for many biochemical assays. The measurements of absorbance, fluorescence, chemiluminescence, and other optical signals can be used to determine various aspects of sample contents [7]. Compared to sophisticated analysis tools, such as nuclear magnetic resonance (NMR) spec-

troscopy and mass-spectrometry, optical measurements are usually faster and cost-effective, although the advanced ones often require fluorescence labeling [8]. In the current work we describe two optical-based procedures for the characterization of extracellular vesicles – lipid concentration measurement using sulfophosphovanillin (SPV) colorimetric assay and application of Raman spectroscopy for the estimation of the overall sample composition and the protein-to-lipid ratio.

Nanoparticle tracking analysis (NTA) is a commonly used method to measure the size of the EVs as well as their concentration [9]. The samples of EVs are intrinsically complex and require rigorous control, thus, additional approaches to the concentration measurement are usually required. For example, the total protein concentration (C_{protein}) is widely used as an indirect measure of the EVs concentration. The protein concentration can be determined using a bicinchoninic acid (BCA) assay [10,11], a Bradford assay, or a multitude of other photometric procedures, such as Qubit assay. These procedures are relatively simple and straightforward. Given that EVs are lipid-based nanoparticles, it seems more relevant to characterise their concentration in terms of lipid concentration. However, measuring the lipid concentration (C_{lipid}) is relatively



challenging; it can be assessed using either the phosphorus assay (determining phosphate concentration in phospholipids) or the SPV assay [12]. The mechanism of the SPV coloring reaction is based on the interaction between the SPV reagent and the alkenyl cation produced from unsaturated lipids during the reaction [13]. In our experience, it has higher sensitivity than the phosphorous assay, so we focus on SPV in the current work. The SPV colorimetric assay can be applied to quantify the lipids extracted from the extracellular vesicles [10,11]; however, only few works have actually described such measurements so far. Many alternative analytical tools can be used for the lipid quantification, including NMR spectroscopy, chromatography, and mass spectrometry [14]. However, in this study we regard only the simplest ones, which rely on the commonly available optical spectroscopy.

Raman spectroscopy is a non-destructive analytical technique that enables the assessment of the chemical composition of samples. It requires a relatively small sample volume (typically ~1–10 μL) and is suitable for the analysis of biological samples [15]. The peaks present in the Raman spectra indicate certain vibration modes of the chemical bonds in the studied samples. Thus, analysis of the spectra provides information about the presence of certain chemical bonds or functional groups in the studied samples, and it can be used to detect specific substances, e.g. low-molecular weight biomarkers [16], pharmaceutical agents [17], toxins [18] and others. Raman spectroscopy can be applied to analyze the samples of extracellular vesicles [19–22]. If combined with specific sample handling procedures and data processing algorithms (primarily, principal component analysis), Raman spectroscopy can distinguish between the EVs isolated from the normal and cancer cells [20]. Besides, Raman spectroscopy can be used to assess the purity of EVs at a semi-qualitative level [21,23]. The advantage of Raman spectroscopy in this context is that it yields information about all the major classes of biomolecules in the samples of EVs based on a minimal sample volume. The sensitivity of Raman spectroscopy can be drastically improved using surface-enhanced Raman spectroscopy (SERS) [24,25]; however this approach requires elaborate sample preparation and increases the overall difficulty of the measurements.

In the current work we describe several steps used to characterize the EVs. Using the EVs from the cell conditioned medium of H358 cell line as a model system, we optimize the SPV assay to measure the contents of lipids in the samples of EVs. Then we analyze the Raman spectra of EVs from different origin to highlight the most typical peaks observed. We compare the Raman spectra obtained from EVs and the lipids extracted from them to confirm the lipid extraction efficacy by the changes in the Raman spectra. Finally, we calculate the ratios of certain peaks in the spectra to estimate the protein-to-lipid ratio. The two described optical assays can help to assess the chemical composition of EVs.

2. Materials and Methods

2.1 Isolation of Small EVs

EV samples were extracted from conditioned cell culture media (H358, A549 and H1299 cell lines), and two body fluids – uterine aspirates obtained from epithelial ovarian cancer patients and gastric juice of healthy individuals. All cell lines were validated by STR profiling and tested negative for mycoplasma.

Cells were cultured in DMEM medium (S420p, Lot #600, PanEco, Moscow, Russia) supplemented with 10% fetal bovine serum (FBS) (SV30160.03, Lot #RG20210008, HyClone, Pasching, Austria), penicillin 100 U/mL and streptomycin 100 $\mu\text{g}/\text{mL}$ (PanEco, Russia) in standard conditions (37 $^{\circ}\text{C}$ and 5% CO_2). The serum was previously purified from native vesicles using ultracentrifugation. To do this, under sterile conditions, FBS was diluted with DMEM in a ratio of 1:4 and unscrewed at 100,000 $\times g$ overnight at 4 $^{\circ}\text{C}$. The resulting supernatant was used to prepare EV-depleted media. To collect the conditioned medium, the cells were seeded into six 175 cm^2 culture flasks, the next day the medium was replaced with EV-depleted DMEM. Once the cells reached 90% confluency, the medium was collected, pooled, and used to isolate EVs. The clinical specimens were received from “N. N. Blokhin National Medical Research Centre of Oncology” of the Ministry of Health of the Russian Federation, diluted in 5 mL of ice-cold phosphate-buffered saline (PBS) and processed no more than two hours after the sampling. After thorough vortexing, samples were consecutively centrifuged at 300 $\times g$, 800 $\times g$ and 2000 $\times g$ for 15 minutes (4 $^{\circ}\text{C}$) to remove cells and cellular debris. After that stage, large vesicles were sedimented at 10,000 $\times g$ for 30 minutes (4 $^{\circ}\text{C}$) and obtained supernatant was frozen and kept at -80°C until needed.

We slightly modified a standard protocol of differential centrifugation described in article [26]. On the first step of preparation, 140 mL of media was centrifuged at 800 $\times g$ and 2000 $\times g$ for 15 minutes (4 $^{\circ}\text{C}$), and the pellet was discarded. The obtained supernatant was subjected to another centrifugation round at 10,000 $\times g$ for 30 minutes (4 $^{\circ}\text{C}$) to clear our samples from apoptotic bodies and large vesicles. Then, we performed first ultracentrifugation round on cleared supernatant at 110,000 $\times g$ (4 $^{\circ}\text{C}$) for 2 h with a SW-28 swinging bucket rotor (k factor 245.5; Beckman Coulter, Brea, CA, USA). The obtained pellet (containing mostly small EVs) was resuspended in 5 mL of ice-cold PBS and centrifuged again at 110,000 $\times g$ (4 $^{\circ}\text{C}$) for 1 h with a SW-50.1 swinging bucket rotor (k factor 154.5; Beckman Coulter). The final pellet was resuspended in 120 μL of ice-cold 10 mM PBS, aliquoted in 2 mL tubes (Protein LoBind #022431005, Lot #J189243G, Eppendorf, Hamburg, Germany), frozen in liquid nitrogen and stored at -80°C for further analysis using transmission electron microscopy (TEM), SPV assay, and Raman spectroscopy. The protocol for isolating EVs from clinical samples was

the same except that before ultracentrifugation, the samples were diluted in 30 mL ice-cold PBS.

The following protocol was used to more rigorously separate vesicles by size. After 2000 ×g step, supernatant was centrifuged at 8000 ×g for 30 minutes (4 °C) to eliminate largest particles. Then, medium extracellular vesicles (mEVs) were sedimented at 19,000 ×g for 1 h (4 °C) and diluted in 120 μL of ice-cold PBS. The acquired supernatant was used to isolate cleared small extracellular vesicles (sEVs) according to the protocol described above.

2.2 Nanoparticle tracking Analysis and Data Processing

The size distribution and concentration of EVs were determined by NTA using a NanoSight LM10 HS instrument (Malvern Panalytical Ltd, Malvern, UK) equipped with a NanoSight LM14 unit with onboard temperature control (Malvern Panalytical Ltd., Malvern, UK), a LM 14C (405 nm, 65 mW) laser unit and a high-sensitivity camera with a scientific CMOS sensor (C11440-50B, Hamamatsu Photonics, Hamamatsu City, Japan). All measurements were performed in accordance with ASTM E2834–12(2018), with the following camera and video processing setups optimized for EV measurement: Camera Shutter = 1500, Camera Gain = 500, Lower Threshold = 195, Higher Threshold = 1885, Screen Gain = 10 and Detection Threshold = 8 (Multi). Each sample was diluted with particle-free PBS down to a concentration of about 1.5×10^8 particles/mL. Twelve videos 60 s long each were recorded and processed using NTA software 2.3 build 33 (Malvern Panalytical Ltd.). The results from all measurements were combined to obtain a particle size histogram and the total particle concentration corrected for the dilution factor using the NTA software feature.

2.3 TEM Imaging and Image Processing

Before imaging, all samples were diluted in PBS to reach a concentration close to 2×10^{11} particles/mL to ensure optimal surface density of particles in sight. The TEM grids coated with formvar and carbon (FCF200-CU-50, Electron microscopy sciences, Hatfield, PA, USA) were treated for 45 s using an Emitech K100X glow discharge device (Quorum Technologies Ltd., Laughton, UK) to make the carbon surface hydrophilic and increase the adsorption of the vesicles. The samples ($V \sim 5\text{--}10$ μL) were deposited onto grids for 2 minutes, stained with 1% uranyl acetate twice for 2 minutes, and then dried. Images were obtained via JEM-1400 (JEOL, Ltd., Akishima, Japan) equipped with the Rio-9 camera (Gatan Inc., Pleasanton, CA, USA) operating at 120 kV. Image processing was performed using ScanEV software (<https://bioeng.ru/scanev/>) [5] and ImageJ (ver. 1.53c, <https://imagej.net/ij/>) [27].

2.4 Lipid Extraction Protocol

The extraction mixture consisted of chloroform (Chimmed, Moscow, Russia) and methanol (Chimmed,

Moscow, Russia) at a 2:1 ratio by volume [28]. The ratio of the sample volume and the extraction mixture was 1:3 [29].

We added 25 μL of the sample to the 75 μL mixture of chloroform and methanol, then vortexed it for 60 s and incubated for 15 min at room temperature. After incubation, 15 μL of water was added, and the solution was vortexed and centrifuged for 15 min at 1000 ×g (20 °C). The chloroform fraction was withdrawn and used for further analysis.

2.5 SPV-assay Protocol for Lipid Quantification

To quantify the content of lipids in the samples of extracellular vesicles, the method of sulfophosphovanillin assay (SPV) was applied to their extracts. The phosphovanillin reagent was a 17% solution of phosphoric acid (Chimmed, Moscow, Russia) with a vanillin (Dr.Bakers, Moscow, Russia) concentration of 1 mg/mL. A solution of lipids in chloroform (either standard or the extract obtained from the EVs) was added to test tubes (Costar, Thermo Fisher Scientific, Waltham, MA, USA) and dried at 90 °C. Then, 160 μL of 96% H₂SO₄ (Component-reactiv, Moscow, Russia) was added to each tube and heated at 90 °C for 10 minutes, then the tubes were cooled at 4 °C for 5 minutes. At the final stage, 160 μL of the phosphovanillin reagent was added to the tubes. The solutions were mixed using a vortex and incubated at 37 °C for 30 minutes. After incubation, the contents of each tube were placed into the wells of a 96-well plate, and the absorbance was measured using a Hidex Chameleon plate reader (Lablogic Systems Limited, Sheffield, UK) at a wavelength of 546 nm. This allowed us to measure the mean mass of the lipids using a calibration curve. The concentration was calculated by dividing the mass over the sample volume used for the lipid extraction ($V_s = 25$ μL).

2.6 Raman Spectroscopy

Raman spectra were obtained using INTEGRA Spectra (NT-MDT, Zelenograd, Russia) instruments at an excitation laser wavelength of 532 nm, diffraction grating 600 lines per mm, objective 20×, laser power 5 mW, spectral range from 600 to 3050 cm⁻¹, spectral resolution 4 cm⁻¹. Either aluminum foil or a mirror glass was used as the substrate. Raman spectra were recorded from dried samples of EVs, as well as lipid extracts from them. When preparing the samples, they were dried on the surface to enhance the Raman signal by successively applying several drops of 2 μL to the same area. Typical spectrum accumulation time was ~30–60 s after 60 s of photobleaching with the same laser power to decrease the fluorescence background. At least three spectra were collected for every sample from the edge of the drop. Baseline subtraction was performed using Spectragryph free software (ver. 1.2) (<https://www.ffmpeg2.de/spectragryph/>).

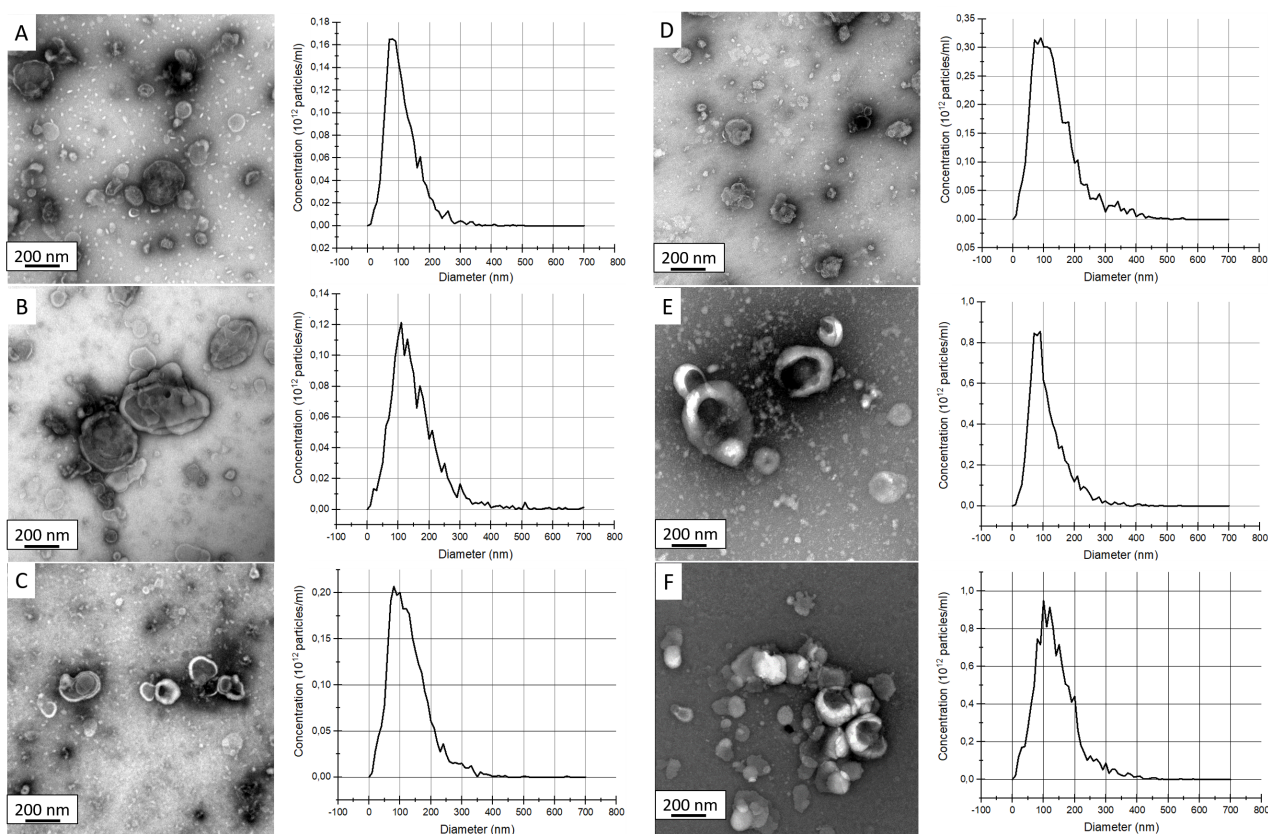


Fig. 1. The TEM images demonstrating the “cup-shaped morphology” (left panel) and the NTA size distributions of the studied extracellular vesicles (right panel). (A,B) sEVs and mEVs isolated from H358 cell line conditioned media, respectively. (C,D) sEVs isolated from A549, H1299 cell line conditioned media, respectively. (E,F) sEVs isolated from uterine aspirate and gastric juice, respectively. The scale bar is 200 nm. sEVs, small extracellular vesicles; NTA, nanoparticle tracking analysis; mEVs, medium extracellular vesicles; TEM, transmission electron microscopy.

2.7 Qubit Protein Assay

Quantitative determination of proteins was carried out using the Qubit 4 fluorimeter (Thermo Fisher Scientific, Waltham, MA, USA) according to the Qubit protein assay protocol provided by the manufacturer. For one measurement, we used 1–3 μL of sample; each sample was measured in triplicate.

3. Results and Discussion

3.1 Overall Characterization of EVs

As evidenced by NTA measurements, all the samples of EVs contained submicron particles. The sizes of these particles are summarised in Table 1. TEM measurements with negative staining revealed the presence of cup-shaped particles in all the studied samples (representative images are shown in Fig. 1). This morphology helps to distinguish between the EVs and some submicron contaminants that are frequently present in the samples [4–6].

The most significant findings presented in the following section were obtained using the two subpopulations of extracellular vesicles (EVs) derived from H358 cells as the model system. The isolation of the EVs was conducted

using a stepwise centrifugation process, whereby the relatively large particles were sedimented at $19,000 \times g$, while the relatively small particles were sedimented at $100,000 \times g$. The latter sample contains the sEVs, and the former one was regarded as a population of relatively large particles called mEVs. Fig. 1A,B illustrates the results of TEM imaging and NTA characterisation of the sEVs and mEVs isolated from H358 cells. The mean size of the mEVs (148 ± 17 nm) was approximately 1.5 times larger than the mean size of the sEVs (108 ± 17 nm). This difference was evidently a consequence of the interplay between the particle size and its tendency to pellet at a specific centrifugal force.

3.2 SPV Colorimetric Assay

We adopted the protocol for assessing the concentration of lipids in the samples of sEVs, as described in [11]. The protocol indicated that the phosphovanillin reagent (PV) should be used at 17% of phosphoric acid, with a volume ratio of sulfuric acid to the PV reagent should of 2:1. However, we observed absorbance was low, prompting us to vary the concentration of the SPV reagent (17% or 68%) and proportions of sulfuric acid and the PV reagent (1:1 or 1:9) to enhance the assay sensitivity [30].

Table 1. The list of the studied samples and their size distribution parameters determined using NTA.

Sample	Mean diameter (NTA) \pm (99%) CI, nm	Median diameter, nm	Mode, nm
H358 sEVs	108 \pm 17	97	87
H358 mEVs	148 \pm 17	132	103
A549 sEVs	124 \pm 8	112	92
H1299 sEVs	131 \pm 16	115	93
Uterine aspirate sEVs	110 \pm 14	93	82
Gastric juice sEVs	138 \pm 26	126	125

CI, confidence interval.

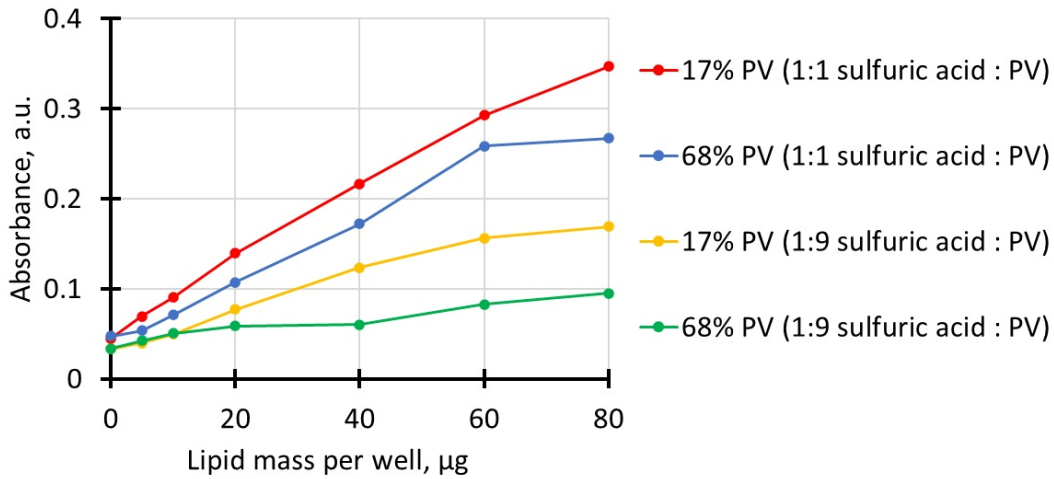


Fig. 2. SPV assay calibration curves. The absorbance was measured at $\lambda = 546$ nm. PV, phosphovanillin; SPV, sulfophosphovanillin.

Fig. 2 shows the calibration curves obtained using the same lipid samples and the different variations of the assay. The lipid mixture used as the mass standard (341602G, Avanti Polar Lipids, Alabaster, AL, USA) contains approximately 70% of unsaturated lipids, so the mass of the lipid per well was calculated by multiplying the mass of the standard by a factor of 0.7. It turned out that the highest colorimetric signal was obtained when the 17% phosphoric acid was used, as recommended in [11,13]. However, the ratio of sulfuric acid to PV was selected at 1:9, as suggested in [31].

The SPV assay is sensitive to the type of vials used for the reaction [10]. We found that the reaction yielded a higher signal when performed in Costar tubes than in Eppendorf Safelock tubes (data not shown). This difference could be due to the subtle variations in the plastic composition and the roughness of the inner surface of the tubes.

We used the SPV assay to measure the concentration of lipids in the samples of sEVs and mEVs isolated from the culture medium of H358 cells (Fig. 1A,B). SPV assay yielded $C_{SPV\ sEVs} = 0.34 \pm 0.2$ mg/mL and $C_{SPV\ mEVs} = 0.4 \pm 0.2$ mg/mL. The measurement errors were relatively large because the absolute amount of lipids was low, and the measurements were carried out at the lower part of the assay dynamic range.

Let us roughly estimate the concentration of lipids in the samples based on their concentration C_{EVs} measured us-

ing NTA. If the mean diameter d of the particles is known, we can estimate the lipid concentration as

$$C_L = C_{EVs} N_L M_L = C_{EVs} M_L \frac{\pi (d^2 + (d - 2\Delta)^2)}{S_L} \quad (1)$$

In this formula N_L and M_L are the mean number of lipid molecules in a particle and the mean molecular weight of a lipid molecule (expressed in Da), S_L is the typical area occupied by a single molecule in a bilayer, and Δ is the membrane thickness. For example, if we use $d = 100$ nm, $\Delta = 5$ nm, $M_L = 744$ Da, $S_L = 0.7$ nm² [32], we get $N_L \cong 81000$, which is an estimate of the number of lipids in a liposome.

We assume that all the vesicles can be characterized by the same M_L and S_L . In this case, for a sample of vesicles characterized by a distribution $C_{EVs}(d)$, we get

$$C_L = \pi \frac{M_L}{S_L} \int C_{EVs}(x) (x^2 + (x - 2\Delta)^2) dx \quad (2)$$

This is an upper-bound estimate for C_L , because the membranes are composed of proteins as well as lipids. Assume that the mass fraction of proteins in a membrane is $\alpha = 0.4$ [33], all the membrane proteins are transmembrane, they have a mean molecular weight of $M_p = 100,000$ Da

and occupy a typical area of $S_p = 7 \text{ nm}^2$ in the membrane. In this case we get

$$C_L = \pi \frac{M_L}{\left(s_L + 2S_P \frac{N_P}{N_L}\right)} \int C_{EV_s}(x) (x^2 + (x - 2\Delta)^2) dx \quad (3)$$

where the molar ratio of proteins and lipids in the membrane is

$$\frac{N_P}{N_L} = \frac{M_L}{M_P} \frac{\alpha}{1 - \alpha} \quad (4)$$

These formulae can be used to estimate the concentration of lipids in the samples of the two subpopulations of EVs isolated from the H358 cells (sEVs and mEVs, Fig. 1A,B). These estimations are based on the NTA data; we replaced integration with sum and obtained $C_{L \text{ sEVs}} = 0.26 \text{ mg/mL}$ and $C_{L \text{ mEVs}} = 0.43 \text{ mg/mL}$. These data are close to the values obtained using the SPV assay: $C_{SPV \text{ sEVs}} = 0.34 \pm 0.2 \text{ mg/mL}$ and $C_{SPV \text{ mEVs}} = 0.4 \pm 0.2 \text{ mg/mL}$. The difference $C_{SPV \text{ sEVs}} < C_{SPV \text{ mEVs}}$ is confirmed by the $C_{L \text{ sEVs}} < C_{L \text{ mEVs}}$ estimates.

One of the studied samples of sEVs obtained from gastric juice (Fig. 1F) had a relatively high concentration of 1.2×10^{12} particles/mL according to NTA and a relatively high concentration of lipids $C_{SPV \text{ GJ}} = 1.2 \pm 0.2 \text{ mg/mL}$ according to the SPV assay. Based on the formula (2), one could expect a lipid concentration of $C_{L \text{ GJ}} = 2.8 \text{ mg/mL}$.

The discrepancy between the theoretical estimate C_L and experimental result C_{SPV} can originate from several factors. First, the SPV assay is sensitive to the non-saturated C=C bonds, and ignores the saturated lipids. Thus, the concentrations C_{SPV} resemble only a fraction of the total sample lipids. Second, Eqn. 1 implies perfect lipid extraction efficacy, which is unlikely to be the case in practice. The loss of lipids during extraction contributes to the discrepancy between C_{SPV} and the actual concentration of lipids in the sample. Third, the assumptions used to estimate C_L can be violated. Particularly, we assumed that the fraction of proteins in the membrane $\alpha = 0.4$ is fixed, which is obviously an oversimplification. Finally, the concentrations C_L can be incorrect due to the artifacts related to the NTA measurements (low sensitivity for the smallest particles, aggregation of some particles). Despite these factors, the resulting values are similar, thereby confirming the overall consistency of our approach. The SPV assay can be a valuable tool for the quantification of EVs in diverse samples, the identification of various sub-populations of EVs (small EVs, ectosomes, apoptotic bodies etc.), and the comparison of EVs isolated from the different origins. The precise quantification of EVs will, in turn, facilitate the determination of their physiological functions and diagnostic potential.

According to the previously published data [10], the SPV assay demonstrated the best performance at $C_{\text{lipid}} > 0.05 \text{ mg/mL}$. In the current work, the SPV assay could detect approximately $1 \mu\text{g}$ of lipids per well. If the experiment is conducted in triplicate, a total of $3 \mu\text{g}$ of lipids is required. Assuming that the lipids were isolated from $V_s = 25 \mu\text{L}$ of sample, this would correspond to a minimum detectable concentration of $C_{SPV} = 0.12 \text{ mg/mL}$. Assuming $d = 100 \text{ nm}$, $C_L = C_{SPV} = 0.12 \text{ mg/mL}$, and using Eqn. 1, we get approximately $C_{EVs} \sim 10^{12}$ particles/mL. This is consistent with the typical concentration of EVs required for the assessment using the SPV assay.

3.3 Raman Spectroscopy of Extracellular Vesicles and Lipid Extracts

From a chemical perspective, extracellular vesicles are multicomponent entities comprising a variety of high-molecular-weight substances (lipids, proteins, nucleic acids) in addition to small molecules. To assess the chemical composition of EVs, we used Raman spectroscopy. The Raman spectra obtained from the sEVs of the different origins (uterine aspirate and conditioned cell culture media of H1299 and A549 cell lines, Fig. 1C–E) are compared in Fig. 3.

At a glance, the most prominent peaks are $\sim 1000 \text{ cm}^{-1}$ (phenylalanine), 1300 cm^{-1} (CH_2 twisting), $\sim 1450 \text{ cm}^{-1}$ (CH_2 deformation vibrations), 1650 cm^{-1} (C=C and Amide I) and the wide peak at $2850\text{--}3000 \text{ cm}^{-1}$. The observed spectra are generally similar to those previously described in the literature for sEVs derived from other sources, including blood serum [20] and cell culture media [15,23,34]. Some sEVs, for example those isolated from the uterine aspirate (Fig. 3A), demonstrated several additional strong peaks at 730 and 790 cm^{-1} , which can be attributed to nucleic acids. Furthermore, the spectra exhibit peaks of high intensity in the regions $1200\text{--}1280 \text{ cm}^{-1}$ and $1580\text{--}1680 \text{ cm}^{-1}$, usually referred to as Amide III and Amide I. In this case, we propose that these changes can be related to higher non-vesicular protein concentration in the sample (according to the Qubit assay, the protein concentration was 1.3 mg/mL).

A typical spectrum obtained from the sEVs produced by A549 cells is presented below (Fig. 4A), and the following peak annotations are listed in Table 2 (Ref. [35–39]). The proteins manifest themselves in the Raman spectra by a number of peaks, and two of them are the most intense. The first one is the Amide I peak, which is centered around $1650\text{--}1660 \text{ cm}^{-1}$. It corresponds to the stretching vibration of the C=O bond in the -CONH- group [40,41]. The second one is a narrow peak at $\sim 1000 \text{ cm}^{-1}$. It corresponds to the characteristic vibrations of the aromatic ring in the aromatic amino acids, mainly phenylalanine. The other protein peaks in the Amide III region ($1230\text{--}1270 \text{ cm}^{-1}$) are relatively weak, although detectable (Table 2). The nucleic acids, although present in the samples of sEVs, yield minor contributions to the Raman spectra [24,25]. For example, in

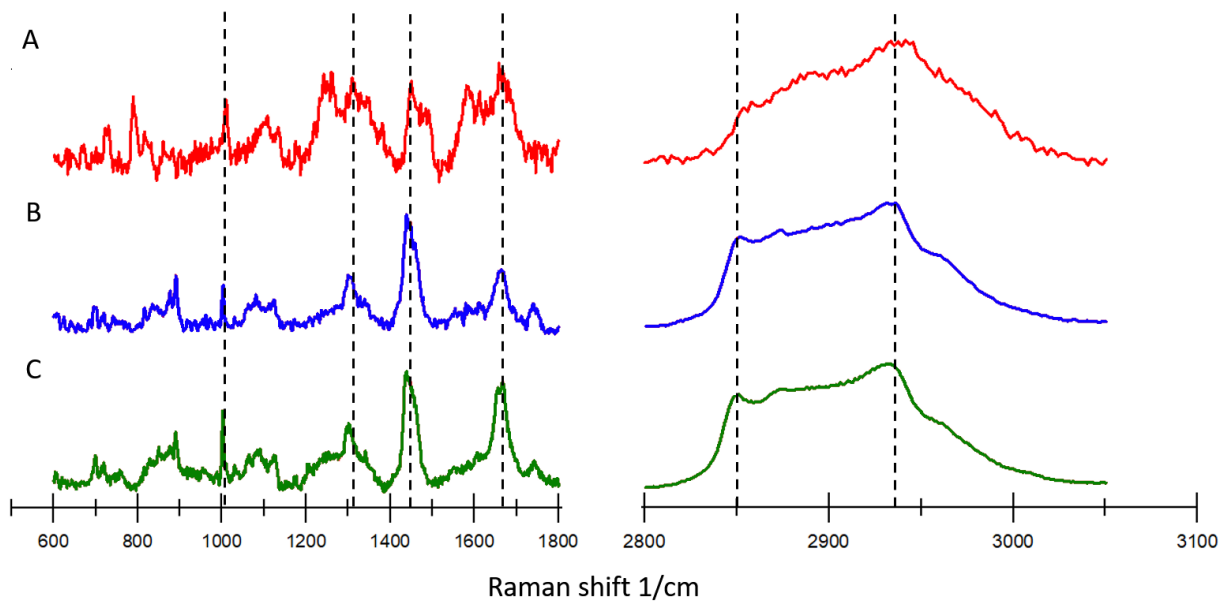


Fig. 3. Raman spectra of the sEVs isolated from the uterine aspirate (A), the cell culture media of H1299 (B) and A549 (C) cells. The key peaks are marked with dotted lines, excitation wavelength $\lambda = 532$ nm.

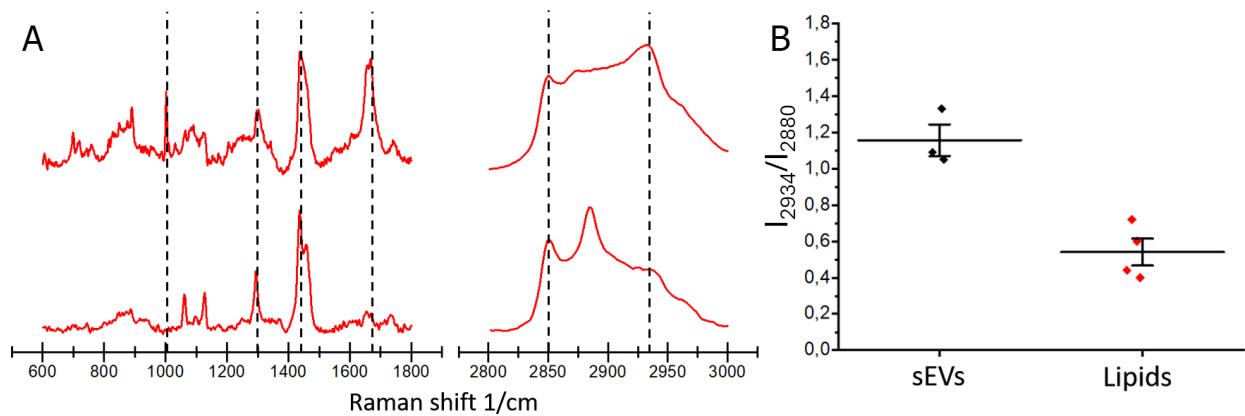


Fig. 4. Raman spectroscopy assessment of the A549 sEVs and the corresponding lipid extract. (A) Raman spectrum of sEVs isolated from conditioned cell culture media (upper row) and Raman spectrum of lipid extracts derived from these sEVs (lower row). The protein-associated peaks were not observed in the spectrum of the lipid extract. Excitation wavelength $\lambda = 532$ nm. (B) The ratios of the I_{2934}/I_{2880} peak intensities.

the spectrum of A549 sEVs, they appeared as small peaks at 785, 810, and 1095 cm^{-1} .

Peaks characteristic of lipids, for example, 1300 cm^{-1} (CH_2 group twisting vibrations), are particularly intense in the spectra of fatty acids [35]. Additionally, the peak at 1740 cm^{-1} , which is associated with the stretching of the C=O double bond, is present in the Raman spectra of triacylglycerides and membrane lipids. The unsaturated lipids have a C=C double bond, and its stretching vibration contributes to the peak in the 1650–1660 cm^{-1} region.

The extraction of lipids from the sEVs and a comparison of spectra can clarify the origin of some peaks. Let us compare the sets of Raman peaks observed in the spectra of A549 vesicles and the lipid extract obtained from them (Fig. 4, Table 2).

The protein-related peaks (amide I peak at 1660 cm^{-1} and the phenylalanine ring peak at ~ 1000 cm^{-1}) were not observed in the spectra of the lipid extracts. There was also a change in the region of 2800–3000 cm^{-1} ; one of the peaks had a lower intensity compared to that of the vesicle spectrum. It was located at 2934 cm^{-1} , which corresponds to the symmetric vibrations of the terminal ($-\text{CH}_3$) group characteristic of some amino acids or triacylglycerides. The ratio of the peak intensities I_{2934}/I_{2880} , is displayed in Fig. 4B. Upon the lipid extraction, there were fewer molecules left in the sample that could contribute to the intensity of the 2934 cm^{-1} peak.

The observed trends are described for the sample of sEVs isolated from the cell culture medium of A549 cells. However, similar trends were observed for the sEVs of

Table 2. Positions of Raman peaks in the spectrum of sEVs isolated from the A549 cells. The peaks were identified based on [35–39]. The rows highlighted in grey correspond to the peaks observed in the spectra of lipid extract obtained from the sEVs.

Raman peak position, cm^{-1}	Interpretation
701–703	Cholesterol ester
720	Choline group
785, 810, 1095	Nucleic acids
752–760, 1360, 1555–1558	Tryptophan
850	Tyrosine
890	C-O-O vibrations
1003	Phenylalanine aromatic ring
1054	C-O and C-N in proteins
1060–1095, 1127	C-C stretching vibrations
1230–1270	Amide III region
1298	CH_2 twisting
1330–1340	Proline lateral chains
1420–1480	CH_3/CH_2 vibrations
1650–1670	C=C, Amide I
1730–1740	C=O ester stretching vibrations
2830–2866	CH_2 symmetric stretching
2870–2890	CH_2 asymmetric stretching
2910–2940	CH_3 symmetric stretching
2940–2967	CH_3 asymmetric stretching

other origin (H358 and uterine aspirate) and the lipid extracts derived from them. We observed the disappearance of the most intensive protein-related peak in the Amide I region. The shape of the double peak at $1436/1455 \text{ cm}^{-1}$ was revealed, as well as that of the lipid-related peak at 1300 cm^{-1} , which became cleaner and narrower. There were also some changes in the region of $2800\text{--}3000 \text{ cm}^{-1}$. The manifestation of the double peak $1436/1455 \text{ cm}^{-1}$ can be attributed to the emergence of the regular packing of the lipid molecules [42]. Overall, the Raman spectra confirmed the efficacy of the lipid extraction procedure.

3.4 Protein-to-Lipid Ratio Quantification

The protein-to-lipid ratio is a useful parameter for the assessment of the purity of the vesicles [19]. This ratio can be calculated by measuring C_{protein} and C_{lipid} independently, or alternatively, it can be estimated using optical spectroscopy. Here we compare these two approaches.

We studied the vesicles isolated from H358 cell culture medium by the three methods: Raman spectroscopy, Qubit assay for C_{protein} , SPV assay for C_{lipid} . The former method can be employed to estimate the $C_{\text{protein}}/C_{\text{lipid}}$ ratio using the intensities' ratio of the two peaks corresponding to the protein and the lipid. The amount of protein can be estimated using the signal intensity at 1000 cm^{-1} (phenylalanine) or 1660 cm^{-1} (Amide I); the amount of lipid can be estimated using 1300 cm^{-1} (CH_2 twisting) or 1440 cm^{-1} (CH_3/CH_2 vibrations). The applicability of this an approach is implicitly confirmed by the Raman spectra obtained from the lipid extracts which do not exhibit a peak at 1000 cm^{-1} and have a relatively low intensity peak at

1660 cm^{-1} . For example, the I_{1660}/I_{1440} ratio was used as an estimate for $C_{\text{protein}}/C_{\text{lipid}}$ in [21], the ratio of amide I band ($1600\text{--}1690 \text{ cm}^{-1}$) to the complex peak ($2750\text{--}3040 \text{ cm}^{-1}$) was used in [23]. The latter approach seems controversial, because the most spectrometers usually require a mechanical rotation of the diffraction grid to change the analyzed range from the $1600\text{--}1690 \text{ cm}^{-1}$ to $2750\text{--}3040 \text{ cm}^{-1}$, and it may cause an overall change in the monochromator sensitivity. Therefore, it seems better to select relatively close peaks for comparison.

The shape of the high-frequency region ($2800\text{--}3000 \text{ cm}^{-1}$) can also be used to estimate the $C_{\text{protein}}/C_{\text{lipid}}$ ratio. It was demonstrated using infrared spectroscopy [21] and Raman spectroscopy [43]. Obviously, there is no generally accepted standard procedure for the selection of peaks that are indicative of the protein and the lipid. The interpretation is further complicated by the fact that the most intense peaks (1440 cm^{-1} , 1660 cm^{-1} , $2800\text{--}3000 \text{ cm}^{-1}$) have certain contributions from both lipids and proteins. We compared five ratios which can be used to assess the $C_{\text{protein}}/C_{\text{lipid}}$ ratio for the vesicles isolated from the H358 cells (Fig. 5). Each of the five parameters was correspondingly higher for the sEVs (Fig. 5C) than for the mEVs (Fig. 5B). This indicated that the sEVs sample had a higher $C_{\text{protein}}/C_{\text{lipid}}$ ratio than the mEVs sample. This conclusion was confirmed by the independent measurements of C_{protein} and C_{lipid} using Qubit and the SPV assay. We obtained $C_{\text{protein}}/C_{\text{SPV}} = 0.7 \pm 0.46$ for the sEVs and $C_{\text{protein}}/C_{\text{SPV}} = 0.45 \pm 0.2$ for the mEVs. These values align with the spectroscopic findings, confirming the consistency of the results across different analytical techniques.

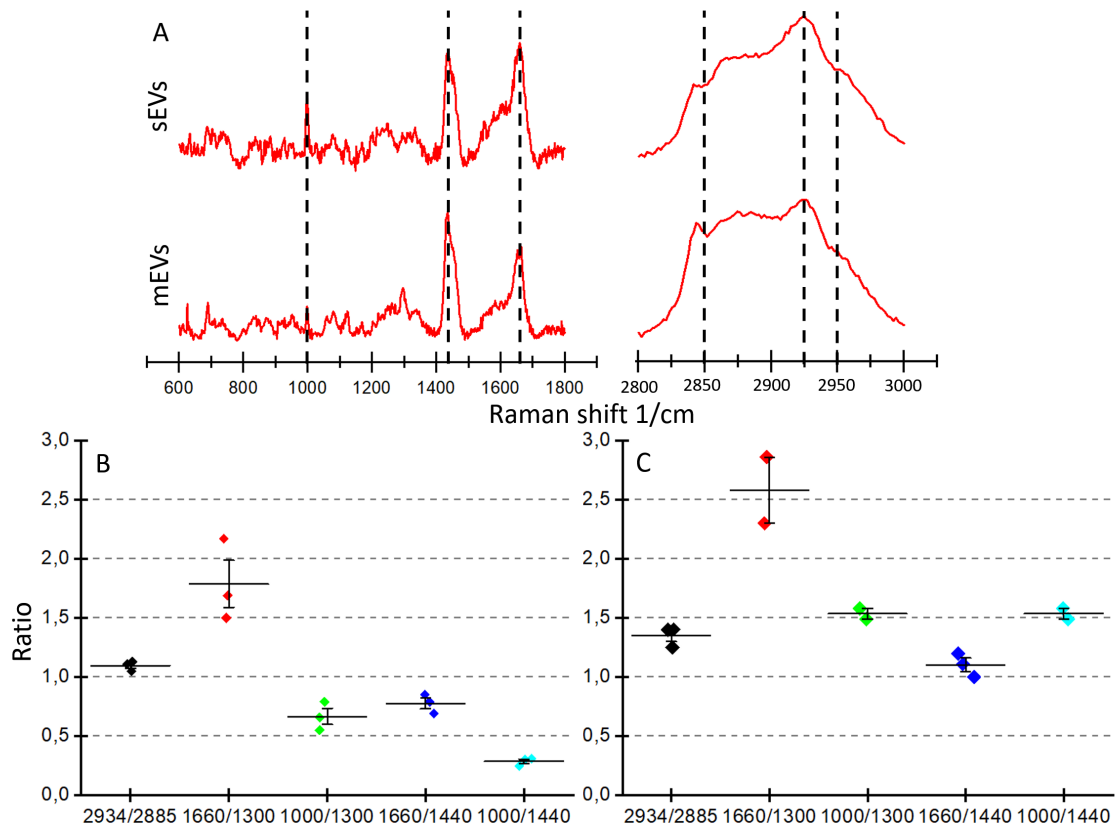


Fig. 5. Raman spectroscopy assessment of the H358 sEVs and mEVs. The Raman spectra of sEVs (upper row) and mEVs (lower row) isolated from the conditioned cell culture media of H358 cells (A). The ratios of the characteristic protein and lipid peaks in Raman spectra of the mEVs (B) and sEVs (C). Excitation wavelength $\lambda = 532$ nm. Each of the five ratios was correspondingly higher for the sEVs (C) than for the mEVs (B).

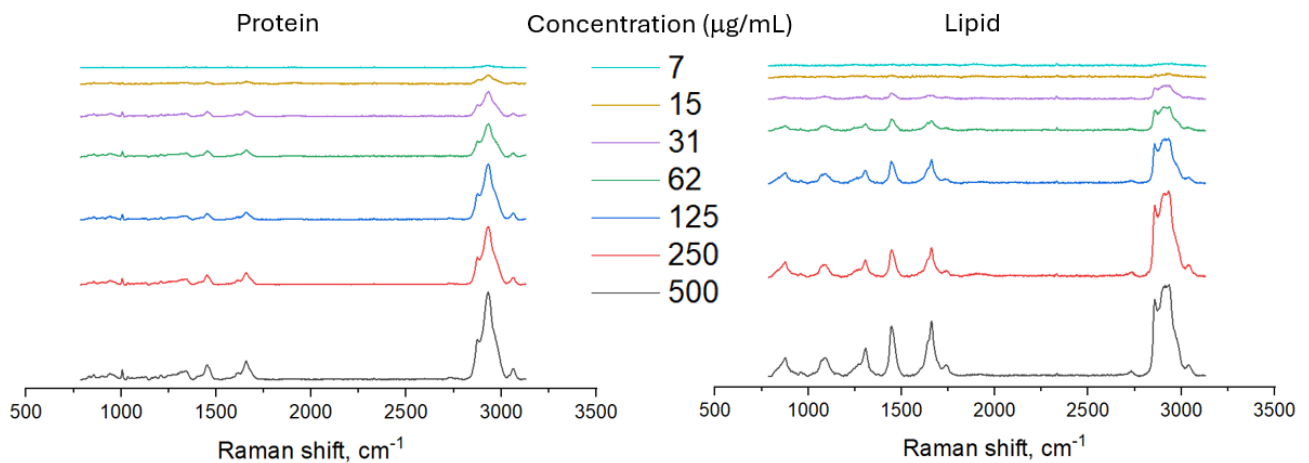


Fig. 6. The Raman spectra of the standard samples of bovine serum albumin (BSA) and liposomes dried on aluminum foil help to estimate of the sensitivity limit.

What is the minimum concentration of sEVs that can be analyzed using Raman spectroscopy? To answer this question, we prepared two standard samples – a pure protein sample bovine serum albumin (BSA) and a sample of

membrane-extruded liposomes made of soy phosphatidylcholine. These two samples were diluted with a two-fold step, deposited onto a substrate and analyzed using Raman spectroscopy. The obtained results are shown in Fig. 6. For

the both samples the most characteristic peaks are barely visible at $\sim 31 \mu\text{g/mL}$ ($\sim 0.5 \mu\text{M}$ for BSA and $\sim 40 \mu\text{M}$ for the lipids) and become almost indistinguishable at $\sim 15 \mu\text{g/mL}$. These figures may be regarded as an estimate of the detection limit of the employed experimental setup. They might be enhanced by using a superior optical system (higher objective aperture, more sensitive detector, etc.) or an improved experimental procedure (larger sample volume used for drop coating deposition, longer signal acquisition). However, the possible enhancement is not expected to be drastic, and similar detection limits were reported by the other authors. For example, Raman spectroscopy was used to obtain spectra from the drops of $1 \mu\text{M}$ lysozyme [44], $3 \mu\text{M}$ insulin [45] or $\sim 10 \mu\text{M}$ synthetic 1,2-dimyristoyl-3-trimethylammonium-propane lipid [46]. Application of SERS can decrease the detection limits further; however, it would also increase the technical complexity of the experiment.

4. Conclusions

Optical measurements are an invaluable tool due to their accessibility and simplicity. They form the basis for a multitude of biochemical assays, ranging from protein concentration assessment to next-generation sequencing. In this study, we employed two measurement procedures, namely the SPV assay and Raman spectroscopy, to assess the properties of EVs.

The SPV assay can be used to measure the concentration of unsaturated lipids in EVs. The detection limit of the assay was $\sim 1 \mu\text{g}$ of lipids per well, which corresponded to $\sim 0.12 \text{ mg/mL}$ of lipids in solution when the experiment was repeated in triplicate. The SPV assay can be employed as a supplementary technique alongside NTA and the protein concentration measurement to determine the concentration of the EVs. These concentration measurements are crucial for the control of the EVs isolation procedures, investigation of their physiological role and diagnostic potential. However, the major drawback of the SPV assay is its focus on the unsaturated lipids.

Raman spectroscopy yielded roughly similar spectra for all the studied samples. However, the sample of sEVs isolated from the uterine aspirate exhibited relatively strong protein-related peaks due to the high protein concentration. The Raman spectra of the EVs were compared with those of the lipids extracted from them. Only the lipid-related peaks were observed in the latter ones, confirming the efficacy of the lipid extraction procedure. Several ratios of peak intensities (I_{2934}/I_{2880} , I_{1660}/I_{1300} , I_{1000}/I_{1300} , I_{1660}/I_{1440} , and I_{1000}/I_{1440}) were used to characterize the $C_{\text{protein}}/C_{\text{lipid}}$ ratio. The aforementioned ratios were higher for the sEVs sample than for the mEVs sample, a finding that was corroborated by the independent measurements of C_{protein} and C_{lipid} .

The detection limit of the Raman spectroscopy was estimated using standard samples of BSA and liposomes. For the both samples the most characteristic peaks are barely

visible at $\sim 31 \mu\text{g/mL}$ ($\sim 0.5 \mu\text{M}$ for BSA and $\sim 40 \mu\text{M}$ for the lipids) and become almost indistinguishable at $\sim 15 \mu\text{g/mL}$. These numbers are in good agreement with the results obtained by the other authors [44–46]. Raman spectroscopy requires a little sample volume ($\sim 1\text{--}10 \mu\text{L}$) and can quickly assess the overall chemical composition of the isolated EVs. However, its major limitation is the sensitivity towards the overall chemical composition, rather than the presence of specific biochemical markers, such as particular proteins (e.g., GPC-1 for pancreatic cancer [47]) or miRNA (e.g., miR-6803-5p for colorectal carcinoma [48]).

The most informative application of Raman spectroscopy in the studies of EVs can rely on several factors. Firstly, the analysis of multiple peaks instead of the individual ones can facilitate the detection of subtle yet meaningful differences between the spectra obtained from the different samples (e.g., the patients and healthy individuals). This analysis can be conducted using specific mathematical procedures, such as principal component analysis [20], orthogonal partial least squares - discriminant analysis [49], or artificial neural networks [34]. Secondly, the sensitivity of Raman spectroscopy is significantly enhanced when utilising the SERS approach. However, this is achieved at the expense of overall experimental complexity [24,25,34]. With further development, Raman spectroscopy can help to classify the EVs and unravel the physiological functions [15,23]. Furthermore, it can become a diagnostic tool, which relies on the assessment of EVs chemical composition [16,20,34].

The samples of EVs are complex and heterogeneous, and their characterization requires different approaches, which rely on both ensemble assessment or single-particle analysis. Optical assessment techniques are an essential tool for the bulk characterisation of samples. The experiential procedures described in this study can help to overcome the challenge of quick and highly informative characterization of the EVs.

Abbreviations

EVs, extracellular vesicle; sEVs, small extracellular vesicles; mEVs, medium extracellular vesicles; SPV, sulfophosphovanillin; NTA, nanoparticle tracking analysis; TEM, transmission electron microscopy; BSA, bovine serum albumin.

Availability of Data and Materials

The raw data (TEM images, Raman spectra, NTA data) are available from the corresponding author upon request.

Author Contributions

AS, ET and DB designed the research study. AS, GS, EP and AP performed the experiments and processed the results. AS, EP and DB analyzed the data. All authors contributed to writing the manuscript and all the authors read

and approved the final manuscript. All authors have participated sufficiently in the work and agreed to be accountable for all aspects of the work.

Ethics Approval and Consent to Participate

Written informed consent has been obtained from the patients or their families/legal guardians to publish this paper. The study was conducted according to the guidelines of the Declaration of Helsinki and approved by the Ethics Committee of N.N. Blokhin National Medical Research Center of Oncology (Ethics Committee Permission Protocol for Project № 22-15-00373 dated 10/06/2022; Approval Protocol №5).

Acknowledgment

The TEM measurements were performed at the User Facilities Center “Electron microscopy in life sciences” at Lomonosov Moscow State University. The Raman spectroscopy measurements were carried out using the equipment purchased on account of the Lomonosov MSU Development Program.

Funding

The work was supported by Russian Science Foundation (project № 22-15-00373).

Conflict of Interest

The authors declare no conflict of interest.

References

- [1] Zhou B, Xu K, Zheng X, Chen T, Wang J, Song Y, *et al.* Application of exosomes as liquid biopsy in clinical diagnosis. *Signal Transduction and Targeted Therapy*. 2020; 5: 144.
- [2] Wang T, Xing Y, Cheng Z, Yu F. Analysis of single extracellular vesicles for biomedical applications with especial emphasis on cancer investigations. *TrAC Trends in Analytical Chemistry*. 2022; 152: 116604.
- [3] Votteler J, Ogohara C, Yi S, Hsia Y, Nattermann U, Belnap DM, *et al.* Designed proteins induce the formation of nanocage-containing extracellular vesicles. *Nature*. 2016; 540: 292–295.
- [4] Sódar BW, Kittel Á, Pálóczi K, Vukman KV, Osteikoetxea X, Szabó-Taylor K, *et al.* Low-Density Lipoprotein Mimics Blood Plasma-Derived Exosomes and Microvesicles during Isolation and Detection. *Scientific Reports*. 2016; 6: 24316.
- [5] Nikishin I, Dulimov R, Skryabin G, Galetsky S, Tchevkina E, Bagrov D. ScanEV - A neural network-based tool for the automated detection of extracellular vesicles in TEM images. *Micron (Oxford, England)*. 2021; 145: 103044.
- [6] Bagrov DV, Adlerberg VV, Skryabin GO, Nikishin II, Galetsky SA, Tchevkina EM, *et al.* AFM-TEM correlation microscopy and its application to lipid nanoparticles. *Microscopy Research and Technique*. 2023; 86: 781–790.
- [7] Haake HM, Schütz A, Gauglitz G. Label-free detection of biomolecular interaction by optical sensors. *Fresenius' Journal of Analytical Chemistry*. 2000; 366: 576–585.
- [8] He Y, Xing Y, Jiang T, Wang J, Sang S, Rong H, *et al.* Fluorescence labeling of extracellular vesicles for diverse bio-applications *in vitro* and *in vivo*. *Chemical Communications (Cambridge, England)*. 2023; 59: 6609–6626.
- [9] Vestad B, Llorente A, Neurauder A, Phuyal S, Kierulf B, Kierulf P, *et al.* Size and concentration analyses of extracellular vesicles by nanoparticle tracking analysis: a variation study. *Journal of Extracellular Vesicles*. 2017; 6: 1344087.
- [10] Osteikoetxea X, Balogh A, Szabó-Taylor K, Németh A, Szabó TG, Pálóczi K, *et al.* Improved characterization of EV preparations based on protein to lipid ratio and lipid properties. *PLoS One*. 2015; 10: e0121184.
- [11] Visnovitz T, Osteikoetxea X, Sódar BW, Mihály J, Lőrincz P, Vukman KV, *et al.* An improved 96 well plate format lipid quantification assay for standardisation of experiments with extracellular vesicles. *Journal of Extracellular Vesicles*. 2019; 8: 1565263.
- [12] Cheng YS, Zheng Y, VanderGheynst JS. Rapid quantitative analysis of lipids using a colorimetric method in a microplate format. *Lipids*. 2011; 46: 95–103.
- [13] Johnson KR, Ellis G, Toothill C. The sulfophosphovanillin reaction for serum lipids: a reappraisal. *Clinical Chemistry*. 1977; 23: 1669–1678.
- [14] Bailey LS, Prajapati DV, Basso KB. Optimization of the Sulfo-Phospho-Vanillin Assay for Total Lipid Normalization in Untargeted Quantitative Lipidomic LC-MS/MS Applications. *Analytical Chemistry*. 2022; 94: 17810–17818.
- [15] Gualerzi A, Niada S, Giannasi C, Picciolini S, Morasso C, Vanna R, *et al.* Raman spectroscopy uncovers biochemical tissue-related features of extracellular vesicles from mesenchymal stromal cells. *Scientific Reports*. 2017; 7: 9820.
- [16] Gulyamov S, Shamshiddinova M, Bae WH, Park YC, Kim HJ, Cho WB, *et al.* Identification of biomarkers on kidney failure by Raman spectroscopy. *Journal of Raman Spectroscopy*. 2021; 52: 1712–1721.
- [17] Vankeirsbilck T, Vercauteren A, Baeyens W, Van der Weken G, Verpoort F, Vergote G, *et al.* Applications of Raman spectroscopy in pharmaceutical analysis. *TrAC trends in analytical chemistry*. 2002; 21: 869–877.
- [18] Mozhaeva V, Kudryavtsev D, Prokhorov K, Utkin Y, Gudkov S, Garnov S, *et al.* Toxins' classification through Raman spectroscopy with principal component analysis. *Spectrochimica Acta. Part A, Molecular and Biomolecular Spectroscopy*. 2022; 278: 121276.
- [19] Mihály J, Deák R, Szigyártó IC, Bóta A, Beke-Somfai T, Varga Z. Characterization of extracellular vesicles by IR spectroscopy: Fast and simple classification based on amide and CH stretching vibrations. *Biochimica et Biophysica Acta (BBA)-Biomembranes*. 2017; 1859: 459–466.
- [20] Russo M, Tirinato L, Scionti F, Coluccio ML, Perozziello G, Riillo C, *et al.* Raman Spectroscopic Stratification of Multiple Myeloma Patients Based on Exosome Profiling. *ACS Omega*. 2020; 5: 30436–30443.
- [21] Zini J, Saari H, Ciana P, Viitala T, Löhmus A, Saarinen J, *et al.* Infrared and Raman spectroscopy for purity assessment of extracellular vesicles. *European Journal of Pharmaceutical Sciences: Official Journal of the European Federation for Pharmaceutical Sciences*. 2022; 172: 106135.
- [22] Xing Y, Cheng Z, Wang R, Lv C, James TD, Yu F. Analysis of extracellular vesicles as emerging theranostic nanoplateforms. *Coordination Chemistry Reviews*. 2020; 424: 213506.
- [23] Gualerzi A, Kooijmans SAA, Niada S, Picciolini S, Brini AT, Camussi G, *et al.* Raman spectroscopy as a quick tool to assess purity of extracellular vesicle preparations and predict their functionality. *Journal of Extracellular Vesicles*. 2019; 8: 1568780.
- [24] Stremersch S, Marro M, Pinchasik BE, Baatsen P, Hendrix A, De Smedt SC, *et al.* Identification of Individual Exosome-Like Vesicles by Surface Enhanced Raman Spectroscopy. *Small (Weinheim an Der Bergstrasse, Germany)*. 2016; 12: 3292–3301.

- [25] Tatischeff I, Larquet E, Falcón-Pérez JM, Turpin PY, Kruglik SG. Fast characterisation of cell-derived extracellular vesicles by nanoparticles tracking analysis, cryo-electron microscopy, and Raman tweezers microspectroscopy. *Journal of Extracellular Vesicles*. 2012; 1: 10.3402/jev.v1i0.19179.
- [26] Théry C. Exosomes: secreted vesicles and intercellular communications. *F1000 Biology Reports*. 2011; 3: 15.
- [27] Schindelin J, Arganda-Carreras I, Frise E, Kaynig V, Longair M, Pietzsch T, *et al.* Fiji: an open-source platform for biological-image analysis. *Nature Methods*. 2012; 9: 676–682.
- [28] Folch J, Lees M, Sloane Stanley GH. A simple method for the isolation and purification of total lipides from animal tissues. *The Journal of Biological Chemistry*. 1957; 226: 497–509.
- [29] Tiphara P, Thongboonkerd V. Differential human urinary lipid profiles using various lipid-extraction protocols: MALDI-TOF and LIFT-TOF/TOF analyses. *Scientific Reports*. 2016; 6: 33756.
- [30] Anschau A, Caruso CS, Kuhn RC, Franco TT. Validation of the sulfo-phospho-vanillin (SPV) method for the determination of lipid content in oleaginous microorganisms. *Brazilian Journal of Chemical Engineering*. 2017; 34: 19–27.
- [31] Eremina MA, Gruntenko NE. Adaptation of the sulfophosphovanillin method of analysis of total lipids for various biological objects as exemplified by *Drosophila melanogaster*. *Vavilov Journal of Genetics and Breeding*. 2020; 24: 441–445.
- [32] Shahane G, Ding W, Palaiokostas M, Orsi M. Physical properties of model biological lipid bilayers: insights from all-atom molecular dynamics simulations. *Journal of Molecular Modeling*. 2019; 25: 76.
- [33] Di L, Artursson P, Avdeef A, Ecker GF, Faller B, Fischer H, *et al.* Evidence-based approach to assess passive diffusion and carrier-mediated drug transport. *Drug Discovery Today*. 2012; 17: 905–912.
- [34] Lee W, Lenferink AT, Otto C, Offerhaus HL. Classifying Raman spectra of extracellular vesicles based on convolutional neural networks for prostate cancer detection. *Journal of Raman spectroscopy*. 2020; 51: 293–300.
- [35] Czamara K, Majzner K, Pacia MZ, Kochan K, Kaczor A, Baranska M. Raman spectroscopy of lipids: a review. *Journal of Raman spectroscopy*. 2015; 46: 4–20.
- [36] Zhu G, Zhu X, Fan Q, Wan X. Raman spectra of amino acids and their aqueous solutions. *Spectrochimica Acta. Part A, Molecular and Biomolecular Spectroscopy*. 2011; 78: 1187–1195.
- [37] Movasaghi Z, Rehman S, Rehman IU. Raman spectroscopy of biological tissues. *Applied Spectroscopy Reviews*. 2007; 42: 493–541.
- [38] Adar F. Interpretation of Raman spectrum of proteins. *Spectroscopy*. 2022; 3: 9–13,25.
- [39] Shipp DW, Sinjab F, Notingher I. Raman spectroscopy: techniques and applications in the life sciences. *Advances in Optics and Photonics*. 2017; 9: 315–428.
- [40] Rygula A, Majzner K, Marzec KM, Kaczor A, Pilarczyk M, Baranska M. Raman spectroscopy of proteins: a review. *Journal of Raman Spectroscopy*. 2013; 44: 1061–1076.
- [41] Kitagawa T, Hirota S. Raman Spectroscopy of Proteins. In Chalmers JM and Griffiths PR (eds.) *Handbook of vibrational spectroscopy* (pp. 3426-3446). John Wiley & Sons, Ltd: Chichester, UK. 2006.
- [42] Boncheva M, Damien F, Normand V. Molecular organization of the lipid matrix in intact Stratum corneum using ATR-FTIR spectroscopy. *Biochimica et Biophysica Acta*. 2008; 1778: 1344–1355.
- [43] Brazhe NA, Popov AV, Parshina EY, Medyanik IA, Yashin KS, Brazhe AR, *et al.* Distinguishing between tumor, infiltrated and normal cortex regions in glioma patients with Raman spectroscopy. *Glia*. 2019; 67: E125–E766.
- [44] Zhang D, Xie Y, Mrozek MF, Ortiz C, Davisson VJ, Ben-Amotz D. Raman detection of proteomic analytes. *Analytical Chemistry*. 2003; 75: 5703–5709.
- [45] Ortiz C, Xie Y, Zhang D, Ben-Amotz D. Proteomic applications of drop coating deposition Raman spectroscopy. *ACS Symposium Series*. 2007; 963: 52–63.
- [46] Šimáková P, Kočíšová E, Procházka M. Sensitive Raman spectroscopy of lipids based on drop deposition using DCDR and SERS. *Journal of Raman Spectroscopy*. 2013; 44: 1479–1482.
- [47] Melo SA, Luecke LB, Kahlert C, Fernandez AF, Gammon ST, Kaye J, *et al.* Glypican-1 identifies cancer exosomes and detects early pancreatic cancer. *Nature*. 2015; 523: 177–182.
- [48] Yan S, Jiang Y, Liang C, Cheng M, Jin C, Duan Q, *et al.* Exosomal miR-6803-5p as potential diagnostic and prognostic marker in colorectal cancer. *Journal of Cellular Biochemistry*. 2018; 119: 4113–4119.
- [49] Bai Y, Yu Z, Yi S, Yan Y, Huang Z, Qiu L. Raman spectroscopy-based biomarker screening by studying the fingerprint characteristics of chronic lymphocytic leukemia and diffuse large B-cell lymphoma. *Journal of Pharmaceutical and Biomedical Analysis*. 2020; 190: 113514.